

INVESTIGATION OF THE EFFECTS OF INITIAL TURBULENCE LEVEL ON THE FLOW FIELD PROPERTIES OF A SUBSONIC JET

Christophe Bogey, Olivier Marsden

Laboratoire de Mécanique des Fluides et d'Acoustique
UMR CNRS 5509, Ecole Centrale de Lyon
69134 Ecully Cedex, France
christophe.bogey@ec-lyon.fr, olivier.marsden@ec-lyon.fr

Christophe Bailly

Same address & Institut Universitaire de France
christophe.bailly@ec-lyon.fr

ABSTRACT

Five round jets at Mach number 0.9 and diameter-based Reynolds number 10^5 originating from a pipe nozzle are computed by Large-Eddy Simulations using grids of 252 million points. In the pipe, the boundary layers are tripped, in order to obtain, at the exit section, laminar mean velocity profiles of momentum thickness equal to 1.8% of the jet radius, and peak turbulence intensities of 0, 3, 6, 9 and 12% of the jet velocity. The influence of initial turbulence on flow development is thus investigated. As the nozzle-exit turbulence level increases, the coherent structures typically found in initially laminar jets gradually disappear, which leads to shear layers spreading at lower rate with strongly reduced rms fluctuating velocities. The jets also develop farther downstream, resulting in longer potential cores.

INTRODUCTION

It has been recognized in the mid-seventies that the effects of the initial conditions are strong in free shear flows, and that they may be one of the reasons of the discrepancies between the data obtained using different facilities. They have consequently been explored in a large number of experiments on axisymmetric mixing layers and jets. The flow and acoustic fields of circular jets have thus been shown, by Hill et al. (1976), Hussain and Zedan (1978a, 1978b), Zaman (1985a, 1985b) and Bridges and Hussain (1987), just to mention a few researchers in this field, to significantly depend on the nozzle-exit flow properties. The momentum thickness δ_θ and the laminar or turbulent state of the boundary layers, and the peak fluctuation intensity with respect to the jet velocity u'_e/u_j have been identified as important parameters. In most experiments, however, their respective influence cannot be clearly distinguished, because they are usually not varying independently if no special attention is paid. Some careful investigations have hopefully been performed on this matter, such as those by Hussain and Zedan (1978a, 1978b), who examined, for both laminar and turbulent initial shear layers, variations

in the momentum-thickness Reynolds number $Re_\theta = \delta_\theta u_j / \nu$ at fixed u'_e/u_j in the former reference, and variations in u'_e/u_j at fixed Re_θ in the latter (ν is the kinematic molecular viscosity). In Hussain and Zedan (1978b), Blasius laminar velocity profiles at $Re_\theta = 200$ with $8.4\% \leq u'_e/u_j \leq 17.2\%$ were especially considered.

The present work, similarly, aims at studying the effects of the initial turbulence on the flow fields of jets at Mach number 0.9 and diameter-based Reynolds number 10^5 , characterized by identical laminar mean profiles at the nozzle exit, but peak fluctuating velocity intensities u'_e/u_j ranging from 0 to 12%. It is the natural continuation of two earlier works on jets at the Mach and Reynolds numbers mentioned above. In Bogey and Bailly (2010), the jet shear layers were initially fully laminar. Their development was found to be strongly dominated by pairings of coherent vortices. In Bogey et al. (2011a), the jets were made initially nominally turbulent by tripping the boundary layers inside a pipe nozzle. Blasius mean velocity profiles of momentum thickness $\delta_\theta/r_0 = 1.8\%$ and peak axial turbulent intensities $u'_e/u_j = 9\%$ were specified at the pipe exit (r_0 is the pipe radius), in agreement with the initial conditions in tripped jets of Zaman (1985a, 1985b). Large-Eddy Simulations (LESs) were carried out using grids containing from 50 to 252 million points. The LES using the finest grid was thus shown to provide shear-layer solutions that are practically grid-converged and, more generally, results that can be regarded as numerically accurate as well as physically relevant. The mixing-layer development in the jet, while exhibiting a wide range of turbulent scales, also displays attenuated but persistent vortex pairings.

In the present paper, LESs of five round jets at Mach number 0.9 and Reynolds number 10^5 , performed at high resolution using grids of 252 million points, low-dissipation schemes and relaxation filtering, are reported. For all jets, laminar mean velocity profiles of momentum thickness $\delta_\theta/r_0 = 1.8\%$, yielding a Reynolds number $Re_\theta = 900$, are imposed inside a pipe nozzle. As for the exit peak turbulence intensities u'_e/u_j , their values are respectively fixed to 0, 3, 6,

9 and 12% by tripping the boundary layers in the pipe. In this way, the influence of initial turbulence level on the jet shear-layer and flow fields is systematically investigated.

PARAMETERS

The main study parameters are given in this section. More details can be found in Bogey et al. (2011a, 2011b).

Numerical methods

The LESs are carried out by solving the 3-D filtered compressible Navier-Stokes equations in cylindrical coordinates (r, θ, z) using low-dissipation, low-dispersion schemes provided in Bogey and Bailly (2004). The axis singularity is taken into account by the method of Mohseni and Colonius (2000). Fourth-order eleven-point centered finite differences are used for spatial discretization, and a second-order six-stage Runge-Kutta algorithm is implemented for time integration. A sixth-order eleven-point centered filter designed in Bogey et al. (2009) to mainly damp the shortest waves discretized is applied every time step to the flow variables. The filtering is also employed as a relaxation filtering (RF), in order to dissipate subgrid-scale energy without significantly affecting the larger scales. This LES-RF approach was developed to avoid the effective flow Reynolds number to be artificially decreased. More information is available in Bogey and Bailly (2006, 2009).

Jet definition

Five isothermal round jets at Mach number $M = u_j/c_a = 0.9$ and Reynolds number $Re_D = u_j D/\nu = 10^5$ are considered (c_a is the speed of sound in the ambient medium, and $D = 2r_0$). The jets originate from a pipe nozzle of radius r_0 and length $2r_0$, with a $0.053r_0$ wide lip. At the pipe inlet at $z = -2r_0$, laminar Blasius boundary-layer profiles of momentum thickness $\delta_\theta = 0.018r_0$ yielding $Re_\theta = u_j \delta_\theta/\nu = 900$, are imposed for the axial velocity.

In four LESs, referred to as Jet3%, Jet6%, Jet9%, and Jet12%, the boundary layers are tripped inside the pipe at $z = -r_0$ ($z = -0.2r_0$ in Jet12%) by adding random vortical disturbances decorrelated in the azimuthal direction. The tripping magnitudes are chosen to obtain exit peak turbulence intensities u'_e/u_j of 3, 6, 9 and 12% in Jet3%, Jet6%, Jet9%, and Jet12%, respectively. In the fifth LES, referred to as Jet0%, no boundary-layer tripping is used in order to deal with an initially fully laminar jet. Note that Jet9% corresponds to the simulation extensively described as Jetring1024drdz in Bogey et al. (2011a).

The nozzle-exit profiles of mean and rms axial velocities calculated in the jets are presented in figure 1. The mean velocity profiles do not appreciably differ from the Blasius profiles fixed at the pipe inlet, leading to exit boundary-layer momentum thicknesses $\delta_\theta(0)/r_0 \simeq 1.8$ and shape factors H around 2.4, as reported in table 1. The peak intensities of velocity fluctuations are also close to 0, 3, 6, 9 and 12% as intended, see in table 1 for the exact values. In Jet9%, in particular, the initial conditions are comparable to those measured in a tripped jet at $Re_D = 10^5$ by Zaman (1985a, 1985b).

As important initial flow features, the integral length scales estimated from axial velocity u'_z in the azimuthal di-

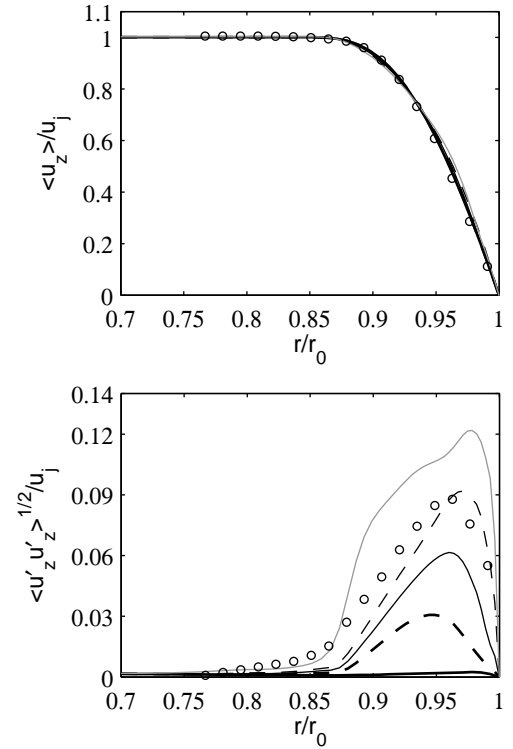


Figure 1. Profiles at $z = 0$ of mean axial velocity $\langle u_z \rangle$ and of the rms values of fluctuating axial velocity u'_z : — Jet0%, - - - Jet3%, — Jet6%, - - - Jet9%, — Jet12%. Measurements: \circ Zaman (1985a, 1985b) for a Mach 0.18, tripped jet at $Re_D = 10^5$.

rection at $r = r_0$ and $z = 0.4r_0$ are collected in table 1. The azimuthal correlation of disturbances just downstream of the pipe lip is high in Jet0%, but rapidly decrease with the exit turbulence level, as previously found in Bogey and Bailly (2010).

Simulation parameters

The LESs are performed using two grids, one in Jet0% for the untripped jet, another in Jet3%, Jet6%, Jet9%, and Jet12% for the tripped jets, both containing $n_r \times n_\theta \times n_z =$

Table 1. Initial jet parameters: boundary-layer momentum thickness $\delta_\theta(0)$, shape factor H , and peak turbulence intensities u'_e at the nozzle exit, and integral length scale $L_{uu}^{(\theta)}$ of velocity u'_z in the azimuthal direction at $r = r_0$ and $z = 0.4r_0$.

	$\delta_\theta(0)/r_0$	H	u'_e/u_j	$L_{uu}^{(\theta)}/r_0$
Jet0%	1.75%	2.55	0.25%	2.059
Jet3%	1.76%	2.52	3.07%	0.104
Jet6%	1.79%	2.48	6.15%	0.020
Jet9%	1.85%	2.36	9.18%	0.013
Jet12%	1.88%	2.33	12.19%	0.010

$256 \times 1024 \times 962 = 252$ million points. They are identical, respectively, to the grids employed for the simulations referred to as *Jetring1024dz* and *Jetring1024drdz* in Bogey et al. (2011a). In the second grid, in particular, the minimum mesh spacings in the radial, azimuthal and axial directions are $\Delta r = 0.36$, $r_0 \Delta \theta = 0.61$ and $\Delta z = 0.72$ per cent of the jet radius, corresponding to 0.20, 0.34 and 0.40 times $\delta_\theta(0)$.

The simulation times are between $325r_0/u_j$ to $375r_0/u_j$. The flow statistics are determined from $t = 175r_0/u_j$, and they are averaged in the azimuthal direction. The computations are finally made using NEC SX-8 computers, at a CPU speed around 36 Gb using OpenMP, and they require up to 7,000 CPU hours each.

RESULTS

The main changes in the jet flow properties when the initial turbulence level varies are illustrated. More results are provided in Bogey et al. (2011b).

Shear flow development

Snapshots of the vorticity norm obtained in the five jets just downstream of the pipe lip are presented in figure 2. For low exit rms velocities in *Jet0%* and *Jet3%*, laminar-turbulent transitions dominated by rolling-ups and pairings of large vortical structures are clearly seen. As u'_e/u_j increases at $z = 0$, the turbulent fields developing in the mixing layers show a wider range of scales, which seems to gradually weaken the above-mentioned mechanisms. For high exit fluctuation levels in *Jet9%* and *Jet12%*, in particular, the jets are initially turbulent, and it is difficult to distinctly observe coherent structures or pairing processes in the shear layers.

The variations over $0 \leq z \leq 10r_0$ of the shear-layer momentum thickness δ_θ are represented in figure 3. As the initial turbulence level raises, the mixing-layer growth begins closer to the exit section, at a position ranging from $z \simeq 1.5r_0$ in *Jet0%* to $z \simeq 0$ in *Jet9%* and *Jet12%*, but it then occurs at a much lower rate. To quantitatively illustrate the latter point, note for instance that the maximum value of the spreading rate $d\delta_\theta/dz$ is 0.045 in *Jet3%*, but only 0.024 in *Jet9%*. The overall development of the jet shear layer is thus found to be slower for higher nozzle-exit velocity fluctuations.

The peak rms values of axial, radial and azimuthal velocities u'_z , u'_r and u'_θ and the maximum Reynolds shear stresses $\langle u'_r u'_z \rangle$ evaluated between $z = 0$ and $10r_0$ are shown in figure 4. In *Jet0%*, maximum intensities around 22% are achieved for all velocity components. The profiles also exhibit dual-peak shapes, which is typical of a first stage of strong vortex pairings in the shear layers according to experimental and numerical data obtained, among others, by Zaman and Hussain (1980) and Bogey and Bailly (2010). As u'_e/u_j increases, the turbulence intensities start to rise farther upstream, but lower peak values are reached. The reduction in rms velocities and Reynolds shear stresses when specifying higher initial disturbances in the shear layers is significant, as shown in table 2. This is however especially the case for u'_r , whose maximum rms values with respect to the jet velocity range from 22.6% in *Jet0%* down to 10.7% in *Jet12%*, while they are of 17.7% in *Jet3%*, 13.7% in *Jet6%* and 11.2% in *Jet9%*. The turbulence intensity profiles finally

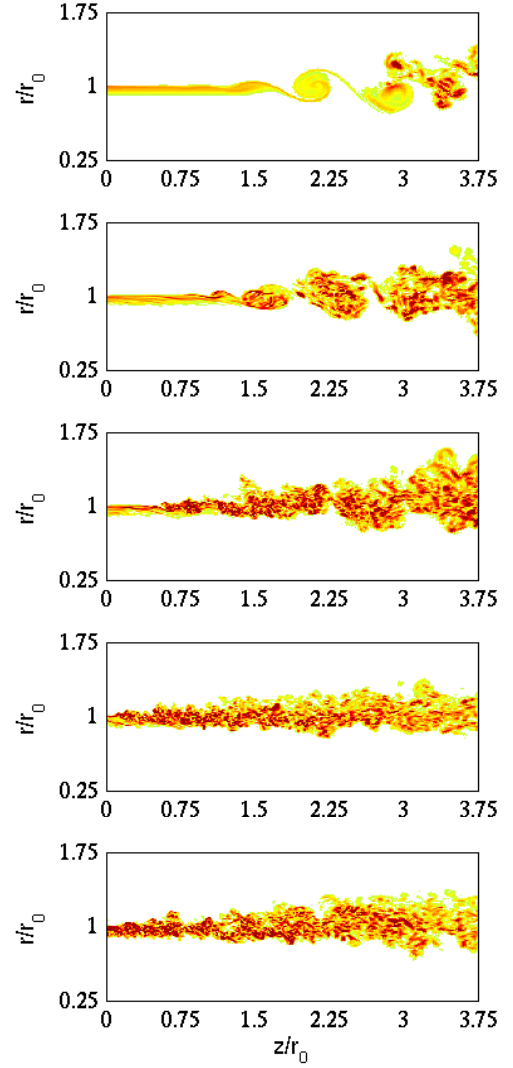


Figure 2. Snapshots in the (z, r) plane of vorticity norm in the shear layer downstream of the pipe lip, from *Jet0%*, *Jet3%*, *Jet6%*, *Jet9%* and *Jet12%*, from top to bottom. The colour scale ranges up to the level of $25u_j/r_0$.

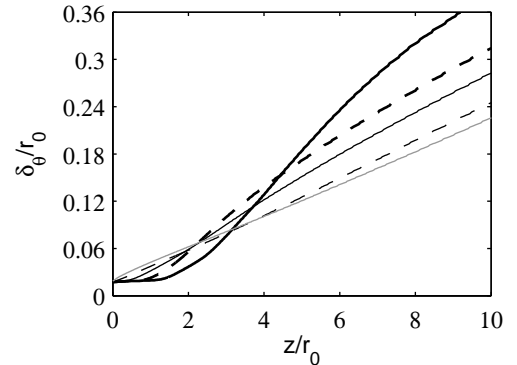


Figure 3. Variations of shear-layer momentum thickness δ_θ : — *Jet0%*, - - - *Jet3%*, — *Jet6%*, - - *Jet9%*, — *Jet12%*.

Table 2. Peak rms values of fluctuating velocities u'_z , u'_r , and u'_θ in the jets, with respect to u_j .

	$\langle u'_z{}^2 \rangle^{1/2}$	$\langle u'_r{}^2 \rangle^{1/2}$	$\langle u'_\theta{}^2 \rangle^{1/2}$
Jet0%	22.7%	22.6%	21.8%
Jet3%	19.9%	17.6%	18.1%
Jet6%	17.7%	13.7%	15.2%
Jet9%	15.4%	11.2%	13%
Jet12%	14.5%	10.6%	12.2%

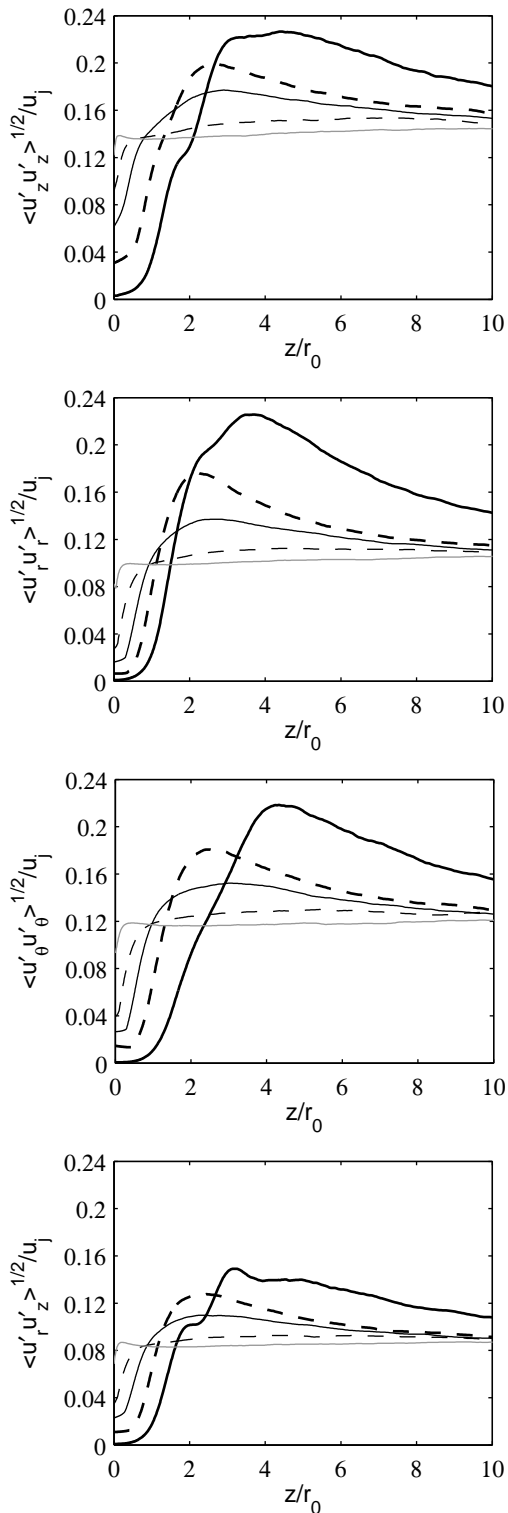


Figure 4. Variations of the peak rms values of fluctuating velocities u'_z , u'_r , and u'_θ , and of the peak magnitudes of Reynolds shear stress $\langle u'_r u'_z \rangle$: — Jet0%, - - - Jet3%, — Jet6%, - - - Jet9%, — Jet12%.

increase nearly monotonically in Jet9% and Jet12%, which is in qualitative agreement with the measurements by Arakeri et al. (2003) in an initially nominally turbulent jet with $u'_e/u_j = 10\%$. They are even quite flat in Jet12%.

The present results demonstrate that the shear-layer development in Reynolds number 10^5 jets becomes gradually and spectacularly smoother when the nozzle-exit turbulence level increases. The peak rms values of velocity obtained for turbulent initial conditions, that are for $u'_e/u_j \simeq 10\%$, are in particular approximately half those for laminar initial conditions. This may be largely due to the strong weakening, if not the disappearance, of the coherent structures and of their mutual interactions in the former case.

Jet flow development

Snapshots of the vorticity norm calculated in the full jets are displayed in figure 5. For higher turbulence intensities at the nozzle exit, the jets appear to develop farther downstream, resulting in longer potential cores. This observation is in agreement with the slower shear-layer growth found in the previous section.

The variations of the centerline mean axial velocity u_c and of the jet half-width $\delta_{0.5}$ are represented in figure 6. As u'_e/u_j raises, the jet mean flow development is delayed since the velocity decay and the jet spreading both start at increasing axial positions. The end of the potential core is thus located at $z_c = 9.3r_0$ in Jet0%, $12.9r_0$ in Jet3%, $14.1r_0$ in Jet6%, $15.9r_0$ in Jet9%, and $17r_0$ in Jet12%, where $u_c(z_c) = 0.95u_j$, as reported in table 3. Downstream of the potential core, the jet development may be more rapid in Jet0%, but it does not seem to strongly differ in the other jets for $u'_e/u_j \geq 3\%$. For the sake of comparison, experimental data available in the literature for jets at Mach number 0.9 and Reynolds numbers higher than 5×10^5 are also plotted in figure 6. It can be noted that they correspond favorably to the results from Jet6%.

In order to finally characterize the jet turbulence, the rms values of the axial and radial fluctuating velocities obtained up to $z = 25r_0$ along the centerline are shown in figure 7. For higher nozzle-exit disturbance level, the peak intensity values are reached farther downstream, in agreement with the delay observed for the mean flow development. They are also reduced for u'_z and u'_r , respectively, from 16.1% and 12.5% in Jet0% down to around 11.5% and 9.3% in Jet9% and Jet12%, refer to table 3. The maximum rms velocities are indeed very

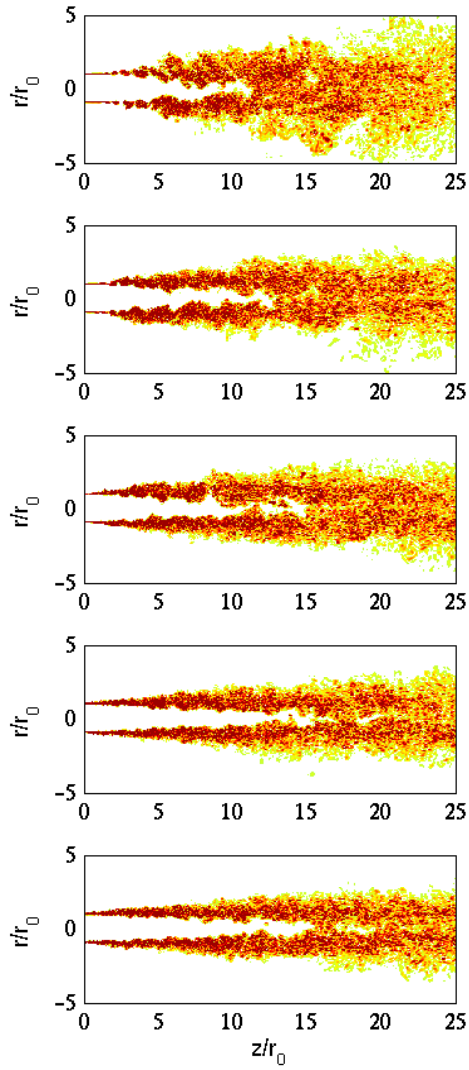


Figure 5. Snapshots in the (z, r) plane of vorticity norm in the full jets up to $z = 25r_0$, from Jet0%, Jet3%, Jet6%, Jet9% and Jet12%, from top to bottom. The colour scale ranges up to the level of $5u_j/r_0$.

similar in the two latter jets, indicating a weak influence of the initial turbulence for $u'_e/u_j \geq 6\%$. The centerline intensity profiles in this case can also be noticed to roughly compare with the scattered measurements obtained for Mach number 0.9 jets at high Reynolds numbers.

CONCLUSION

The LES results presented in this paper show the significant influence of the initial turbulence on the flow fields of jets at Reynolds number 10^5 . The strongest effects are found on the shear-layer features. For low nozzle-exit velocity fluctuations, the mixing layer is clearly dominated by large coherent structures, whose pairings result in a rapid flow development as well as in high turbulence intensities. As the initial disturbances increase, these structures are less and less discernible in the vortical fields, leading to a slower shear-layer spread-

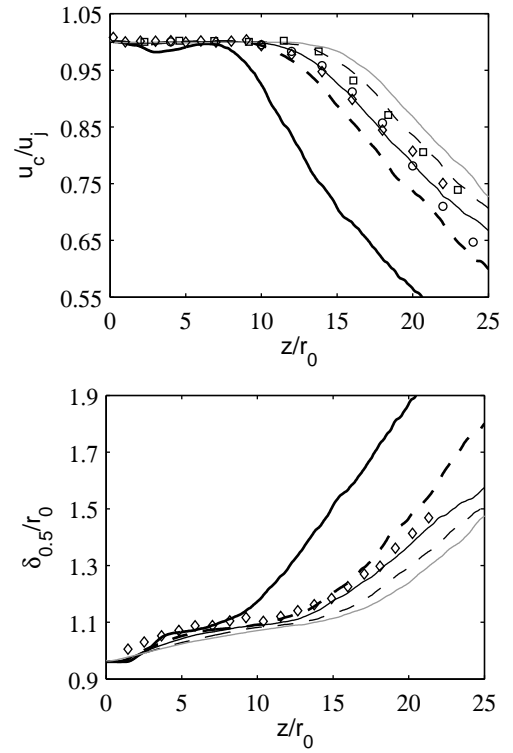


Figure 6. Variations of centerline mean axial velocity u_c and of jet half-width $\delta_{0.5}$: — Jet0%, - - - Jet3%, Jet6%, - . - . Jet9%, — — — Jet12%. Measurements for Mach 0.9 jets at $\text{Re}_D \geq 5 \times 10^5$: \circ Lau et al. (1979), \square Arakeri et al.(2003), \diamond Fleury et al. (2008).

ing and to an important reduction in rms velocity values. The impact of initial turbulence on the overall jet flow is less spectacular. The main modification when specifying higher u'_e/u_j at $z = 0$ consists of the lengthening of the potential core. For $u'_e/u_j \geq 3\%$, in particular, the downstream jet development seems to be merely delayed without further notable change.

Table 3. Axial position of the end of the potential core z_c , and peak rms values of fluctuating velocities u'_z and u'_r on the jet axis.

	z_c/r_0	$\langle u_z'^2 \rangle^{1/2} / u_j$	$\langle u_r'^2 \rangle^{1/2} / u_j$
Jet0%	9.3	16.1%	12.5%
Jet3%	12.9	12.4%	10%
Jet6%	14.1	12.4%	9.3%
Jet9%	15.9	11.4%	9.4%
Jet12%	17	11.5%	9.2%

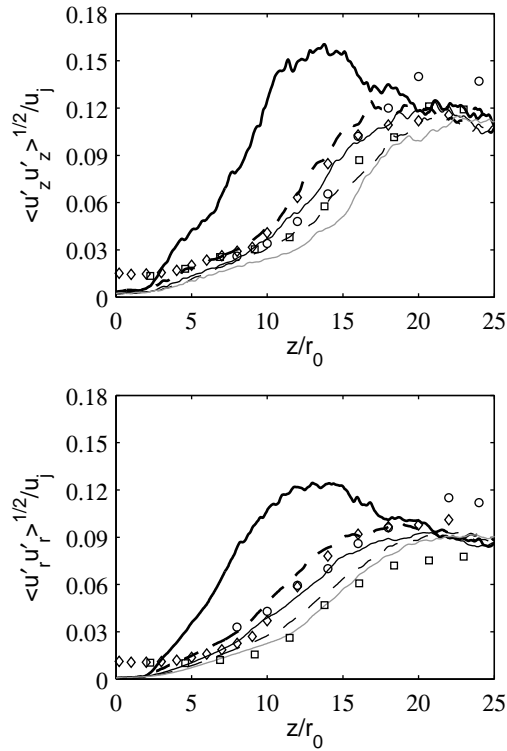


Figure 7. Variations of centerline rms values of fluctuating velocities u'_z and u'_r : — Jet0%, - - - Jet3%, — Jet6%, . . . Jet9%, — Jet12%. Measurements for Mach 0.9 jets at $Re_D \geq 5 \times 10^5$: \circ Lau et al. (1979), \square Arakeri et al.(2003), \diamond Fleury et al. (2008).

ACKNOWLEDGMENTS

This work was granted access to the HPC resources of IDRIS under the allocation 2010-020204 made by GENCI (Grand Equipement National de Calcul Intensif).

REFERENCES

Arakeri, V.H., Krothapalli, A., Siddavaram, V., Alkisar, M.B., and Lourenco, L., 2003, "On the use of microjets to suppress turbulence in a Mach 0.9 axisymmetric jet," *J. Fluid Mech.*, Vol. 490, pp. 75-98.

Bogey, C. and Bailly, C., 2004, "A family of low dispersive and low dissipative explicit schemes for flow and noise computations," *J. Comput. Phys.*, Vol. 194, No. 1, pp. 194-214.

Bogey, C. and Bailly, C., 2006, "Large Eddy Simulations of transitional round jets: influence of the Reynolds number on flow development and energy dissipation," *Phys. Fluids*, Vol. 18, No. 6, pp. 1-14.

Bogey, C. and Bailly, C., 2009, "Turbulence and energy budget in a self-preserving round jet: direct evaluation using large-eddy simulation," *J. Fluid Mech.*, Vol. 627, pp. 129-160.

Bogey, C., de Cacqueray, N., and Bailly, C., 2009, "A shock-capturing methodology based on adaptive spatial filtering for high-order non-linear computations," *J. Comput. Phys.*, Vol. 228, No. 5, pp. 1447-1465.

Bogey, C. and Bailly, C., 2010, "Influence of nozzle-exit boundary-layer conditions on the flow and acoustic fields of initially laminar jets," *J. Fluid Mech.*, Vol. 663, pp. 507-539.

Bogey, C., Marsden, O., and Bailly, C., 2011a, "Large-Eddy Simulation of the flow and acoustic fields of a Reynolds number 10^5 subsonic jet with tripped exit boundary layers," *Phys. Fluids*, Vol. 23, No. 3, 035104, pp. 1-20.

Bogey, C., Marsden, O., and Bailly, C., 2011b, "A computational study of the effects of nozzle-exit turbulence level on the flow and acoustic fields of a subsonic jet," 17th AIAA/CEAS Aeroacoustics Conference, 6-8 June 2011, Portland, Oregon, USA.

Bridges, J.E. and Hussain, A.K.M.F., 1987, "Roles of initial conditions and vortex pairing in jet noise," *J. Sound Vib.*, Vol. 117, No. 2, 1987, pp. 289-311.

Fleury, V., Bailly, C., Jondeau, E., Michard, M., and Juvé, D., 2008, "Space-time correlations in two subsonic jets using dual-PIV measurements," *AIAA Journal*, Vol. 46, No. 10, pp. 2498-2509.

Hill, W.G., Jenkins, R.C., and Gilbert, B.L., 1976, "Effects of the initial boundary-layer state on turbulent jet mixing," *AIAA Journal*, Vol. 14, No. 11, pp. 1513-1514.

Hussain, A.K.M.F and Zedan, M.F., 1978a, "Effects of the initial condition on the axisymmetric free shear layer: Effects of the initial momentum thickness," *Phys. Fluids*, Vol. 21, No. 7, pp. 1100-1112.

Hussain, A.K.M.F and Zedan, M.F., 1978, "Effects of the initial condition on the axisymmetric free shear layer: Effects of the initial fluctuation level," *Phys. Fluids*, Vol. 21, No. 9, pp. 1475-1481.

Lau, J.C., Morris, P.J., and Fisher, M.J., 1979, "Measurements in subsonic and supersonic free jets using a laser velocimeter," *J. Fluid Mech.*, Vol. 93, No. 1, pp. 1-27.

Mohseni, K. and Colonius, T., 2000, "Numerical treatment of polar coordinate singularities," *J. Comput. Phys.*, Vol. 157, No. 2, pp. 787-795.

Zaman, K.B.M.Q., 1985a, "Effect of initial condition on subsonic jet noise," *AIAA Journal*, Vol. 23, pp. 1370-1373.

Zaman, K.B.M.Q., 1985b, "Far-field noise of a subsonic jet under controlled excitation," *J. Fluid Mech.*, Vol. 152, pp. 83-111.

Zaman, K.B.M.Q. and Hussain, A.K.M.F., 1980, "Vortex pairing in a circular jet under controlled excitation. Part 1. General jet response," *J. Fluid Mech.*, Vol. 101, No. 3, pp. 449-491.